Electrochimica Acta 211 (2016) 879–890

Contents lists available at ScienceDirect

Electrochimica Acta

journal homepage: www.elsevier.com/locate/electacta

# Grafting of 4-pyrrolyphenyldiazonium *in situ* generated on NiTi, an adhesion promoter for pyrrole electropolymerisation?

A. Jacques[a], M.M. Chehimi[b], C. Poleunis[c], A. Delcorte[c], J. Delhalle[a], Z. Mekhalif[a,*]

[a] Laboratory of Chemistry and Electrochemistry of Surfaces (CES), University of Namur, rue de Bruxelles, 61, B-5000 Namur, Belgium
[b] Université Paris-Est, ICMPE UMR 7182 CNRS — UPEC, 2-8 rue Henri Dunant, 94320 Thiais, France
[c] Université catholique de Louvain, Institute of Condensed Matter and Nanosciences (IMCN), Croix du Sud 1, Louvain-la-Neuve, Belgium

ARTICLE INFO

*Article history:*
Received 23 March 2016
Received in revised form 23 May 2016
Accepted 11 June 2016
Available online 18 June 2016

*Keywords:*
Nitinol
*In situ* generated diazonium
electrografting
electropolymerization
pyrrole

ABSTRACT

The present work investigates the grafting of *in situ* generated 4-pyrrolyphenyldiazonium (Py-PD) on NiTi by two different ways. The first way is the electrografting of Py-PD while the second one is the grafting without electrochemistry at room temperature (spontaneous grafting) or under heating (either conventional heating or induction heating). Both modification routes led to the successful grafting of Py-PD. The hypothesis of a cationic intermediate is proposed for the grafting without electrochemistry since it is thermally activated and the oxidized surface of NiTi is not a reductant. For both modification approaches, the $TiO_2$ surface layer of NiTi has been preserved and the NiTi corrosion resistance improved, an important parameter to preserve/improve the NiTi biocompatibility. The second part of the work is dedicated to the electropolymerization of pyrrole on modified surfaces with the Py-PD as adhesion promoter.



## 1. Introduction

Among the various shape memory alloys Nitinol is probably the most investigated. Nitinol stands for *Ni*ckel-*Ti*tanium (the two constituents present in nearly equal percentage of this alloy) and *N*aval *O*rdnance *L*aboratory place of its discovery [1,2]. Due to, its intrinsic properties such as shape memory [3,4], super-elasticity [3,4], high fatigue strength [3,5], non-magnetic [3,5,6], heat and impact resistance [3], resistance to corrosion [3,4], and biocompatibility [3–6], NiTi has become a material of great interest [7], particularly in the biomedical field [3–6]. Its biocompatibility properties result from the presence of a thin protective titanium dioxide surface layer that enhances corrosion resistance and reduces $Ni^{2+}$ release [4,8–11]. Indeed, $Ni^{2+}$ release is problematic due to its cytotoxicity and its carcinogenicity [4,8–12]. Consequently, in recent years, a great deal of attention has been paid to the surface modification of NiTi in order to impart and/or improve surface properties such as biocompatibility [4,8], bioactivity [4] and corrosion resistance [4].

Grafting diazonium salts on metal and alloy substrates is an attractive way for the surface modification of theses substrates and has been thoroughly studied in the past decades [13–17]. Robust films result from the covalent carbon-metal [18–20] and/or carbon-metal oxide [20–23] bonds formed through the process. The diazonium salt grafting is generally achieved by electrochemical [14,24–29] or chemical reduction [21,24,25]. In this last process, a chemical reductant such as hypophosphorous acid [25] can be used as source of electron. Alternartively, spontaneous process [21,24,25,30] (without reducing agent) can be used if the substrate is reducing enough. It is generally admitted that for both, chemical and electrochemical diazonium salt grafting, the process includes aryl radical formation and nitrogen loss resulting from the diazonium salt reduction [14,21,24,25,31]. However, if there is no electron source (no electrochemical grafting, no reducing agent and non-reducing substrate) for the dediazotation, a mechanism involving the grafting of a carbocation instead of a radical aryl is possible [14,24,32–34]. Purification and especially storage of diazonium salts can be problematic given their poor stability. Consequently, since the beginning of the past decade, a one-step procedure including *in situ* diazonium generation from their aniline precursors and their subsequent grafting in the same solution has been actively investigated [13]. The *in situ* generation can be achieved by addition of sodium nitrite ($NaNO_2$) with at least 2 equivalents (eq) of acid (compared to the amount of aniline) [35,36]. Generally, a large excess of acid (at least 8 eq.) which can be detrimental for active metal surface modification is used [14,29]. However recently, the use of gentle conditions for the *in situ* generation of diazonium has been reported [26–28,37].

* Corresponding author.
*E-mail address:* zineb.mekhalif@unamur.be (Z. Mekhalif).

http://dx.doi.org/10.1016/j.electacta.2016.06.060
0013-4686/

In the present work, we investigate a comparative study between, the electrografting and the grafting by conventional heating (CH) or induction heating (IH) of *in situ* generated Py-PD (Fig. 1) as an extension of our previous published work on Ni [27]. CH and IH conditions for the modification of NiTi are used because the spontaneous grafting (i.e. at room temperature) by reduction of the diazonium salt using NiTi surface as chemical reductant is unlikely due to its native thin titanium dioxide surface layer (preventing the use of NiTi as electron source) [4,8–11]. Furthermore, spontaneous grafting of Py-PD on NiTi after its surface polishing (to eliminate the titanium dioxide layer) in a controlled atmosphere is unsuitable to preserve its corrosion resistance and thus its biocompatibility. Nevertheless, as mentioned previously diazonium salt grafting with aryl cation intermediates is possible [14,24,32,33] when thermally activated [24,32]. For this purpose, the magnetic induction heating, based on physical phenomena (Faraday-Lenz law, Eddy currents, and Joule effect) commonly used to heat electrically conductive materials thanks to a time-varying magnetic field is a technique of choice. Indeed, this technique relies on the advantage of heating the surface of the material locally limiting the energy input [38] and without any contact. Induction heating helps the preservation of the solution especially when the chemicals are unstable or reactive, like aryl diazonium salts [39].

The use of grafted diazonium salt as adhesion promoter for the electropolymerisation of conducting polymers is well known [40–43]. Particularly, among the wide variety of monomers to generate conducting polymers, pyrrole is of particular interest mainly because of its relatively low oxidation potential (~0.8 V/SCE). Indeed, electropolymerization process on active metals (such as Ni and Ti) are challenging because of the competition between the oxidation of the monomer and the metal. Furthermore, polypyrrole because of its corrosion inhibitor [44–47] efficiency and its biocompatibility [48–51] is of interest for biomedical applications [48,49,51] such as stimulation of the osteointegration [51–54] and the growth of the endothelial cells [48–50,52,54]. As orthodondic, cardio-vasular and orthopedic implants are the main biomedical applications of NiTi [4,5], its covalent functionalisation with polypyrrole is of great interest. Surprisingly, there is only a few reported works devoted to pyrrole polymerisation on NiTi [55–58], only two references about Py-PD grafting [27,59] and one study about the use of grafted Py-PD as adhesion promoter for the covalent grafting of polypyrrole [59].

The present work after the characterization of electrografted and grafted by CH and IH Py-PD on NiTi investigates the electropolymerization of pyrrole on modified surfaces with the Py-PD as adhesion promoter as schematically shown in Fig. 1.

## 2. Experimental part

### 2.1. Chemicals

Absolute ethanol (VWR Prolabo), sodium nitrite (Sigma-Aldrich, ≥ 99.0%), lithium perchlorate ($LiClO_4$) (Acros, 99%), sodium chloride (Fluka, ≥ 99.5%), acetonitrile (Chem-Lab, HPLC grade), 4-(1H-pyrrol-1-yl)aniline (Maybridge, 97%) (Py-A), perchloric acid (Vel, 70% p.a.), ruthenium (III) hexamine trichloride (Sigma-Aldrich, 98.0%) and potassium sulfate (Acros, 99%) were used without further purification.

### 2.2. Nitinol substrates preparation

Nitinol (Ni 56% – Ti balance) substrates rectangular-shaped plates (20 mm × 10 mm × 0.3 mm), purchased from AMF (Alliage à Memoire de Forme, France), are first mechanically polished down to 1 μm on a Buehler Automet 300 instrument using silicon carbide papers (P1200) and diamond suspension pastes (9, 3 and 1 μm) from Struers.

The NiTi plates are then cleaned in absolute ethanol in a sonication bath for 15 min before being blown dry under nitrogen and stored for further use or analysis. Just before their modification, the substrates are cleaned in absolute ethanol, submitted to UV-ozone for 30 min (Jelight 42-220), and cleaned in absolute ethanol again, before being blown dry under nitrogen and used for analysis or modification.

### 2.3. Electrografting of Py-PD in situ generated from its aniline precursor (Py-A) on the NiTi plates

50.0 mL of 5 mM Py-A and $10^{-1}$ M $LiClO_4$ solution in acetonitrile is mixed with 1 eq. of $NaNO_2$ in presence of 2 eq. (42 μL) or 10 eq.

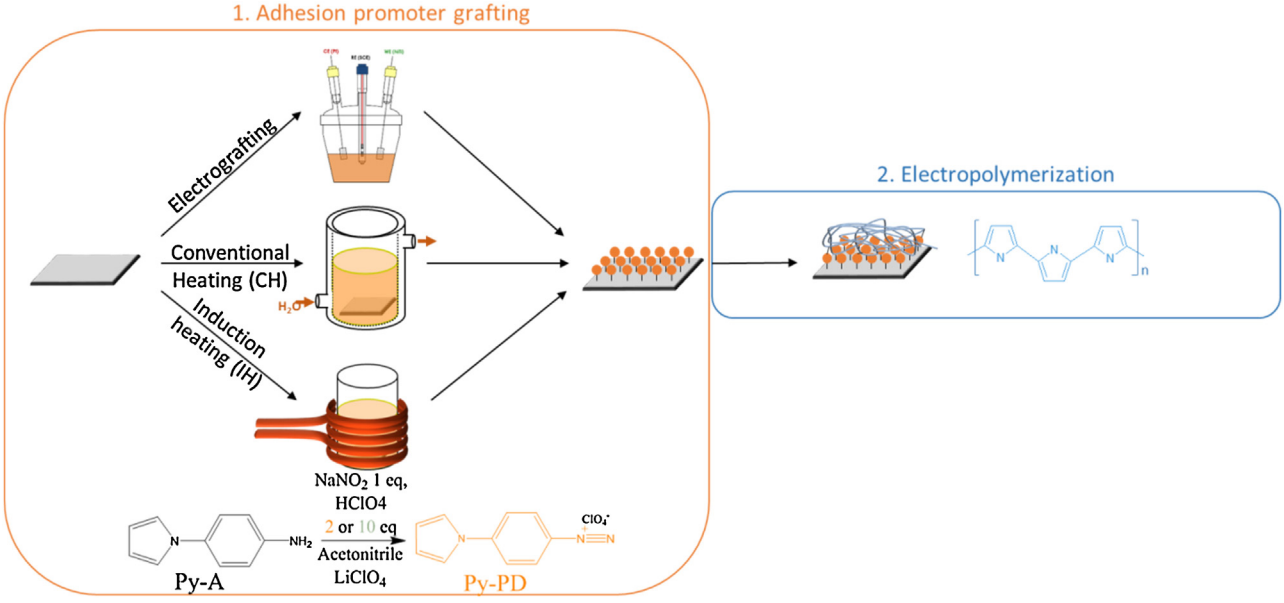


**Fig. 1.** Schematic representation of the work methodology.

(210 μL) of $HClO_4$ (70%) under stirring and nitrogen flow for 45 min. The electrografting is then carried either by cyclic voltammetry (CV) (15 s of equilibration time at 0.5 V/SCE followed by 10 cycles from 0.5 to −1.0 V/SCE at a scan rate of 50 $mVs^{-1}$) or in potentiostatic conditions (-0.9 V/SCE for 10 min). In both cases stirring and nitrogen flow are stopped during the electrografting. In the sequel of this work, substrates electrografted with Py-PD are called NiTi|Py-PD 2 eq or NiTi|Py-PD 10 eq according to the amount of acid used for the diazonium *in situ* generation. A reference sample named NiTi|Py-A is made by applying these electrografting conditions in a Py-A solution without any $NaNO_2$ nor $HClO_4$. After modification, the substrates are cleaned in absolute ethanol under ultrasonication for 15 min before being blown dry under nitrogen and stored before their characterization or modification by the electropolymerization of Py.

All the electrochemical experiments are carried out in a classical three electrodes electrochemical cell with a platinum foil as counter electrode, a saturated calomel electrode (SCE) as reference and a controlled area (1 $cm^2$ using an insulating PTFE scotch tape provided by 3 M as a mask) for the NiTi substrate used as working electrode (WE). The used potentiostat is a Princeton Applied Research Potentiostat/Galvanostat Model Versastat 3 controlled by computer with the Versastudio software.

### 2.4. Thermally assisted grafting of Py-PD in situ generated from its aniline precursor on the NiTi plates

50.0 mL of 5 mM Py-A solution in acetonitrile is mixed with 1 eq. of $NaNO_2$ in presence of 2 eq. (42 μL) of $HClO_4$ (70%) under stirring and nitrogen flow for 45 min. Then, the NiTi substrates are modified by immersion in 10 mL of this solution for 30 min. Three conditions are used either at room temperature referenced as spontaneous (NiTi|Py-PD SP), under induction (NiTi|Py-PD IH) or conventional heating (NiTi|Py-PD CH) at a temperature close to 70 °C and close to 80 °C (IH70/80 and CH70/80 Py-PD respectively) according to the temperature profiles presented on Fig. 2. The graftings are also perfomed in a Py-A solution (without any $NaNO_2$ nor $HClO_4$) and are referenced by the prefix Py-A (in opposition to Py-PD). After modification, substrates are cleaned under ultrasonication in denatured ethanol for 15 min and dried under nitrogen and stored for characterizations.

CH was performed in a thermostatic electrochemical cell. IH was performed with an Ambrell EasyHeat induction heating system with a power output of 206 W or 394 W and a frequency of 198 kHz for the IH70 and IH80 conditions respectively. The used solenoid is composed of 7 loops with an internal diameter of 9 cm. Temperature profile at the surface of the NiTi is measured with a thermocouple K-type welded at its surface and a Keithley 2700 data acquisition multimeter, monitored with a Keithley XLINX 2700 Startup software.

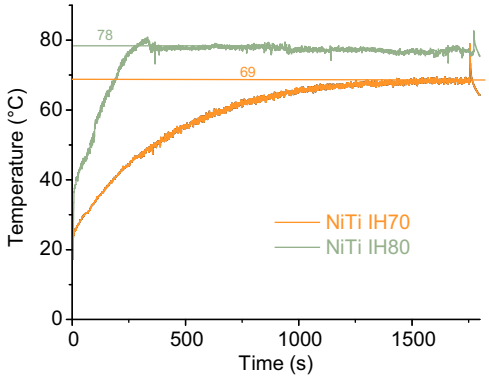


**Fig. 2.** Temperature evolution at the surface of a NiTi substrate heated in 10 mL ACN by induction heating at 70 and 80 °C.

### 2.5. Pyrrole electropolymerization on bare and modifiedNiTi

Electropolymerization of pyrrole is carried out using bare NiTi or NiTi|Py-PD 2eq as working electrode. In the sequel of this work after pyrrole electropolymerization substrates are called respectively NiTi|PPy and NiTi|Py-PD|PPy. The electrochemical medium is acetonitrile containing 0.1 M $LiClO_4$ and 10 mM of pyrrole. Cyclic voltammetry is carried out by sweeping the potential from −1 V to 1.2 V at 50 mV/s during 10 cycles. A CV in a monomer free solution is carried out on bare NiTi and NiTi-Py-PD 2eq substrates to evaluate the impact of the electropolymerization condition. At the end, the substrates are cleaned by ultrasonication in denatured ethanol for 15 min, dried under nitrogen and stored for characterizations. Due to the poor adhesion when submitted to sonication, the pyrrole electropolymerized samples are just copiously rinsed with ethanol before being dried and stored.

### 2.6. Substrate characterization

Bare and modified NiTi substrates are characterized by X-ray Photoelectron Spectroscopy (XPS), Time of Flight Secondary Ion Mass spectroscopy (ToF-SIMS), Polarization Modulation InfraRed Reflection Absorption Spectroscopy (PM-IRRAS), Linear Sweep Voltammetry (LSV), Cyclic Voltammetry (CV) and water static contact angle measurements.

XPS spectra are recorded using a Thermo Scientific K-Alpha spectrometer using a monochromatized X-ray Kα radiation (1486.6 eV), the photoelectrons being collected at 0° with respect to the surface normal and detected with a hemispherical analyzer. The spot size of the X-ray source on the sample is 200 μm and the analyzer is operated with a pass energy of 200 eV for survey spectra and 50 eV for high resolution core levels spectra. The binding energy (BE) of core levels is calibrated against the C1 s BE set at 285.0 eV. The Ti2p peak has a doublet structure and analyzed accordingly. $Ti2p_{3/2}$ and $Ti2p_{1/2}$ spacing depends on the oxidation state of titanium. The corresponding $Ti2p_{3/2}$ and $Ti2p_{1/2}$ binding energies are 454.3 eV and 460.4 eV for Ti (0), 456.0 eV and 460.5 eV for Ti (II), 457.2 and 462.4 eV for Ti (III), 458.8 eV and 464.5 eV for Ti (IV), respectively. Thickness and coverage values for Py-PD coatings are estimated from the collected XPS data. The thickness of a layer material A (i.e. grafted Py-PD) deposited on a bulk material B (i.e. NiTi) can be obtained from the relative attenuation of the B element (Ti2p peak) signal, which is quantified as:

$$\frac{I_B}{I_{B,0}} = \exp\left(-\frac{d_A}{\lambda_{B,A}}\sin\theta\right)$$

where $I_B/I_{B,0}$ is the ratio of the bulk element B peak intensities (modified surface/bare surface), $d_A$ the layer material A thickness, $\lambda_{B,A}$ the bulk material B photoelectrons mean free path through layer material A, and θ the takeoff angle (here θ = 0°) [21,60].

Time of flight secondary ion mass spectrometry (ToF-SIMS). Chemical characterisation of samples were carried out by using ToF-SIMS. An IONTOF V instrument (IONTOF, GmbH, Münster, Germany) was used. A pulsed $Bi_5^+$ metal ion source was used to produce a primary beam using an acceleration voltage of 30 kV. An AC target current of 0.11 pA with a bunched pulse width lower than 1.2 ns was used. Both positive and negative secondary ion species were analysed. For spectra, a raster of 128 × 128 data points over an area of 500 × 500 $\mu m^2$ was used. The total primary ion beam dose for each analysed area was always kept below 2 $10^{10}$ ions.$cm^{-2}$, ensuring static conditions. Lateral resolution of ~3 μm and mass resolution m/Δm >5000 at 29 m/z were maintained for positive and negative spectra acquisition. Charge compensation was done by interlaced electron flood gun ($E_k$ = 20 eV). All data analyses were

carried out using the software supplied by the instrument manufacturer, SurfaceLab (version 6.5).

Polarization modulation infrared reflection absorption spectroscopy data are collected from a Bruker Equinox55 PMA37 equipped with a liquid-nitrogen-cooled mercury–cadmium–telluride (MCT) detector and a zinc-selenide photoelastic modulator. The measurements are carried out with the photoelastic modulator set at half-wave retardation of 2600 $cm^{-1}$. The infrared light, reaching the sample surface at an angle of 80°, is modulated between s- and p-polarization at a frequency of 50 kHz. As the sample is analyzed via reflection from the air/Ni substrate surface interface, and as the substrate also has a higher index of refraction than air, there is a surface selection rule that only allows the component of a vibration's transition dipole moment perpendicular to the metal surface to be detected. Therefore only the p-polarized wave contributes to the absorption signal [61]. Signals generated from each polarization (Rs and Rp) are detected simultaneously by a lock-in amplifier and used to calculate the differential surface reflectivity ($\Delta R/R = (Rp - Rs)/(Rp + Rs)$). The spectra are taken by collecting 512 scans at a spectral resolution of 2 $cm^{-1}$.

Electrochemical techniques (CV and LSV) provide information on the grafted Py-PD layers quality. The cell used enables an analysis of a well-defined and reproducible spot (0.28 $cm^2$) on the sample.

Linear sweep voltammetry is carried out in a 0.5 M sodium chloride solution, after being degassed 10 min under nitrogen flow, by sweeping the potential from −1 to 1 V/SCE at 1 $mVs^{-1}$.

CV using a redox probe made of $Ru(NH_3)_6Cl_3$ 5 mM in a 0.1 M $K_2SO_4$ solution is used to evaluate the relative blocking properties of the modified electrode, which are inversely proportional to its electroactivity. Cyclic voltammograms are recorded from −0.05 V to −0.85 V to 0.45 V/SCE with a scan rate of 20 mV/s for 1 cycle. The parameter $I_{rel}$ (%) = $(Ipa_{film}/Ipa_{bare})*100$ ($Ipa_{film}$ = current density of the anodic peak of modified electrode and $Ipa_{bare}$ = current density of the anodic peak of bare substrate) is used to assess qualitatively the electrode coverage and the electron transfer rate [29,62].

CV are carried out in a 0.1 M $LiClO_4$ solution in acetonitrile by sweeping potential values from −1 V to 1 V at 50 mV/s to achieve doping dedoping cyclic voltammograms for substrates modified by electropolymerization of pyrrole.

Water static contact angle measurements are carried out at room temperature on a DIGIDROP (GBX Surface Science Technology) contact angle goniometer. A syringe is used to dispense 2 μL of probe droplets of milli-Q water on the sample surface.

Peeling test (ASTM D3359) on modified NiTi were also carried out in order to assess the adhesion of the formed organic layers. This test consists in scratching the modified sample with a metallic comb with spacing streaks of 1 mm (Elcometer 1542), then a scotch-tape is stuck on the scratched sample and removed. XPS analysis of the peeled portions of the coating produced by the peeling test provides normalized informations on the adhesion character of the layer.

Each surface modification has been repeated at least three times for each characterization method in order to assess the reproducibility of the results.

## 3. Results and discussions

Fig. 1 displays the different steps and methodology of the work. The results will be thus presented in two main parts. First, the modification of NiTi via diazonium *in situ* generated grafting (either electrografting or thermally activated grafting). Second, the electropolymerization of pyrrole and the role of the grafted Py-PD as adhesion promoter.

### 3.1. Electrografting of Py-PD on NiTi

Cyclic voltammograms recorded in Py-A/acetonitrile solution in absence of any other reactants (Fig. 3a) clearly present a capacitive current without any Faradic contribution indicating the absence of any reaction at the electrode. It confirms the absence of Py-PD and previous results recorded on Ni [27]. CVs recorded in the 2 eq *in situ* generation condition (Fig. 3a) shows at the first cycle a broad cathodic reduction peak centered at −0.600 V. For the 10 eq condition (Fig. 3b) the reduction peak (-0.765 mV) at more cathodic potential is broader and a current density one order of magnitude higher than for the 2 eq case. As previously discussed for Ni [27] this difference between the CVs peak (shape and intensity) is related to the concomitant diazonium salt and proton reduction (which are in higher concentration for the 10 eq condition). In both cases 2 and 10 eq, a current density decrease starting from the 2nd cycle and a complete disappearance of the cathodic peak at the 10th cycle indicate the passivation of the electrode by an organic layer via the electrografting of diazonium [29]. From these CV experiments, the lowest electrografting potential recorded for a reduction peak is at −0.765 V (in the 10 eq. condition). Based on these experiments, in the sequel of this work the electrografting of *in situ* generated Py-PD is carried out in potentiostatic condition at a more cathodic potential of −0.9 V for 600 s in order to ensure the diazonium grafting.

The XPS survey and C1s, N1 s core level spectra for electrografted organic films by potentiostatic conditions in each of the studied acidic conditions (2 or 10 eq of $HClO_4$) are presented in Fig. 4.

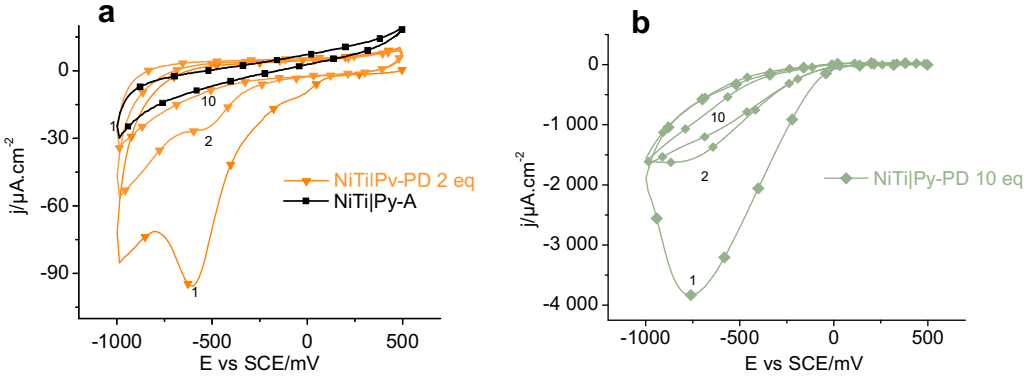


**Fig. 3.** Cyclic voltammograms (1st, 2nd and 10th cycles) obtained for NiTi|Py-A and NiTi|Py-PD 2eq (-▼-) (**a**) and NiTi|Py-PD 10 eq (-♦-) (**b**).

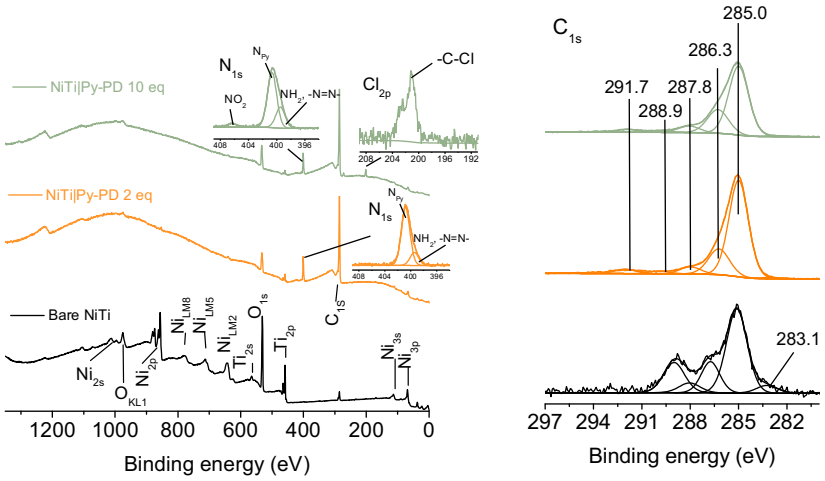


**Fig. 4.** XPS survey and core level spectra of N1s, Cl2p (left part) and XPS core level spectra of C1 s (right part) for bare NiTi, NiTi|Py-PD 2 eq and NiTi|Py-PD 10 eq.

The survey spectra (Fig. 4) of the modified substrate in both acidic conditions (2 and 10 eq. of $HClO_4$) show an increase of C1 s and N1 s peaks intensity compared to bare NiTi which confirms the presence of an organic layer. Indeed, the increase of C1 s and N1 s peak intensity is due to the presence of the electrografted Py-PD layer. More information are obtained from the core level spectrum. The C 1 s spectra can be analyzed with five different components (Fig. 4). The peak at 283.1 eV typical of carbide type carbon atoms [19] and therefore carbon atoms involved in a C-Ni or C-Ti binding. The more intense, centered at 285 eV, is attributed to aliphatic and aromatic carbon atoms. The peaks at 286.3 eV is characteristic of carbon atoms involved in C-O functions but also in C-N and C=N bonds [45,63]. Finally, the components centered at 287.8 eV and 288.9 eV are characteristic of oxidized carbon species i.e. carbonyl group (C=O) and carboxylic functions (C=O-OH), respectively. The carbon present on bare NiTi substrates is attributed to adsorbed atmospheric contamination. The components centered at 283.1 eV is absent from the spectrum of Py-PD grafted samples (for both acidic conditions) while a decrease of highly oxidized carbon components (i.e. carbonyl and carboxylic) is observed and a shake-up component characteristic of aromatic compounds appears at 291.7 eV [64]. This shake-up component confirms the successful electrografting of the Py-PD on NiTi surface for both acidic conditions.

The N1 s peaks (Fig. 4) for NiTi|Py-PD 2 eq can be fitted with two components. The first at 399.4 eV is attributed to the nitrogen of the amine function ($NH_2$) of the aniline, nitrogen of atmospheric contamination ($N_2$) or nitrogen of azo bridges (C—N=N-C) [21,65]. The component at 400.6 eV is characteristic of nitrogen in a pyrrole function (NPy) [27,63]. For the NiTi|Py-PD 10 eq sample an unreproducible additional component can be observed at 406.3 eV due to a nitro function [21,66]. This result indicates a nitration of the grafted Py-PD for some samples in presence of 10 eq of $HClO_4$. A nitration requests the presence of $NO_3^-$ and is catalyzed in presence of a strong acid [35,67,68] but also in presence of nitrosonium ions [67]. The first one is present and the nitrosonium is generated in the modification bath. Normally, $NO_3^-$ is absent from the modification media but its generation by disproportionation of nitrous acid as described in equation 1 [69] can be hypothesized. Furthermore, photocatalyzis of this reaction by $TiO_2$ (which is the main component at the NiTi surface) nanoparticles has been reported [70].

$$(HNO_2 + H^+ + e^- \rightleftharpoons NO + H_2O)X2 \quad E^\circ = 0.983\ V/SHE$$

$$\underline{(NO_3^- \pm 3H^\pm \pm 2e^- \rightleftharpoons HNO_2 \pm H_2O)X\text{-}1} \quad \underline{E^\circ = 0.934\ V/SHE}$$

$$3\ HNO_2 \rightleftharpoons 2NO + NO_3^- + H^+ + H_2O \quad (1)$$

Another particular observation for NiTi|Py-PD 10 eq is the presence of a peak at 201.0 eV characteristic of chlorinated aromatics is observed [71]. Chlorination requests the presence of $Cl_2$ and Lewis acid in the reaction media [35]. $Li^+$ is a Lewis acid and the generation of $Cl_2$ due to the oxidation of nitrous acid by perchloric acid can be hypothesized (equation 2) [69]. This reaction induces also the generation of $NO_3^-$ which is a reactant for the nitration reaction.

$$(ClO_4^- + 8H^+ + 7e^- \rightleftharpoons 1/2Cl_2 + 4H_2O)X2 \quad E^\circ = 1.39$$

$$\underline{(NO_3^- \pm 3H^\pm \pm 2e^- \rightleftharpoons HNO_2 \pm H_2O)X\text{-}7} \quad \underline{E^\circ = 0.934}$$

$$7HNO_2 + 2ClO_4^- \rightleftharpoons 7NO_3^- + Cl_2 + 5H^+ + H_2O \quad (2)$$

To the best of our knowledge these two side-reactions (i.e. nitration and chlorination) during the *in situ* generation of a diazonium salts have never been reported. Indeed, the conditions for the *in situ* generation are gentle (even when 10 eq of $HClO_4$ are used) compared to the concentrated acidic mixture generally used for the nitration. It follows that $NO_3^-$ and $Cl_2$ should be present in quite low amount in order to avoid the side graft reactions. Nevertheless, Py-PD is particular since it is a highly conjugated diazonium salt which could lead to a better stabilization of the Wheland intermediate generated during the aromatic electrophile substitution.

It can be concluded than beyond the interest to use gentle acidic condition (i.e. 2 eq of $HClO_4$) for the *in situ* generation of diazonium salts to avoid detrimental effect on the surface of sensitive oxidizable metal (which are not observed here since the electrografting of Py-PD with 10 eq of $HClO_4$ has been successfully achieved). This condition allows avoiding side-reaction during the grafting of diazonum salts. Hence, the 2 eq acid condition should be generalized or at least used when the diazonium *in situ* generation is problematic.

XPS spectra of $Ti_{2p}$ can be analyzed (Fig. 5) using 4 doublets with $Ti2p_{3/2}$ component centered at 454.3 eV, 456.0 eV, 457.2 eV

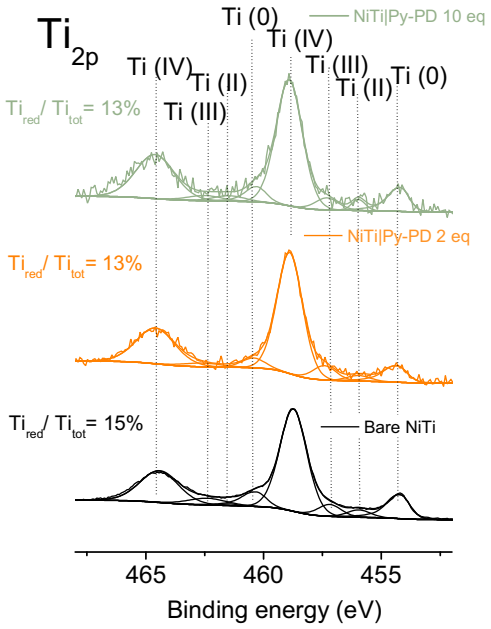


**Fig. 5.** XPS core level spectra of Ti2p for bare NiTi, NiTi|Py-PD 2 eq and NiTi|Py-PD 10 eq substrates.

and 458.8 eV corresponding to Ti (0), Ti (II), Ti (III) and Ti (IV) oxidation states, respectively [72]. The $Ti_{red}/Ti_{tot}$ ratio is equal to 15% for bare NiTi and 13% for both NiTi|Py-PD 2 and 10 eq. These results are strong supporting evidence for the preservation or reinforcement of the titanium oxides surface layer. Despite the fact that the surface composition of NiTi is complex and depends of the surface treatment, it is mainly composed of $TiO_2$ with some amount of Ni inclusions [8–11]. This implies the presence of a Ni-rich ($Ni_3Ti$) sublayer under the $TiO_2$ surface layer of which depth and exact composition is related to the extreme surface layer composition [4,11]. Therefore, it is reasonable to hypothesize the formation of C-O-M and C—N=N-O-M covalent bonds between the grafted molecule and the Nitinol substrate. Indeed, even if the presence of C-O-M bonds is difficult to demonstrate, these bonds have already been evidenced [21,23] even on $TiO_2$ [22].

To further assess the interfacial bond nature, TOF-SIMS experiments of both NiTi|Py-PD 2 eq and NiTi|Py-PD 10 eq have been performed. These results confirm the presence of C—N=N-O-M bonds (observation of negatively charged fragment of $NiCN_2O^-$, $NiC_2N_2O^-$ and $NiC_4N_2O^-$) but also of C—N=N-M bonds (observation of negatively charged fragment of $NiC_2N_2^-$, $NiC_4N_2^-$ and $NiC_6N_2^-$). Surprisingly, fragments containing titanium are not observed. This absence does not allow to exclude the presence of bonds involving titanium since it can be due to a poor ability of these fragments to ionize. Furthermore, the covalent grafting of diazonium on titanium and the presence of C-O-Ti bonds has been reported [22].

The intensity ratios calculated on the basis of the XPS analysis (Table 1) confirm that nitrogen present on NiTi|Py-A samples comes from small amount of physisorbed aniline precursor. Indeed, the $N_{Py}/N_{NH2}$ ratio is equal to 1 and the very low NPy/(Ni + Ti) (0.04) ratio is indicative of a low coverage of the NiTi surface. Furthermore, the important $C/N_{Py}$ (21.8) ratio shows that the main part of the carbon comes from atmospheric contaminations and not of physisorbed Py-A. In contrast, XPS ratios indicate the electrografting of the *in situ* generated PD-Py for both acidic conditions (C/(Ni + Ti) $\geq$ 46.1 and NPy/(Ni + Ti)$\geq$ 4.6). The over-estimated $C/N_{Py}$ ratio (10.8 and 10.7 for NiT|Py-PD 2 and 10 eq respectively compared to 10 according to the Py-PD stoichiometry) is due to the presence of atmospheric contaminations. The $N_{Py}/N_{NH2}$ ($\geq$ 2.2) ratio describes some aniline precursor trapped on the grafted organic film or the formation of azo bridge (both amine function and azo bridge having the same binding energy cf.supra) due to an incomplete dediazotation. Nevertheless, this $N_{Py}/N_{NH2}$ ratio is at least equal to 2.2 which indicates that a dediazotation occurs even if it is partial and if aniline precursor is trapped in the film, it is in small amount. The fact that dediazotation occurs corroborate the hypothesis of C-O-Ti bond formation between the electrografted layer and the NiTi surface. The presence of Ti oxides as main constituent of the NiTi surface is highlighted by the Ti/(Ni + Ti) ratio (at least equal to 0.72) and its preservation or reinforcement after the diazonium grafting is confirmed (lower ratio for bare compared to modified NiTi). The high coverage (the high C/(Ni + Ti) and $N_{Py}$/(Ni + Ti) ratios) observed for the two tested conditions indicates the formation of a multilayer film in line with previously reported diazonium grafting studies [14,21,30]. These results are also in agreement with the calculated thickness for the electrografted films 9.0 ± 1.7 nm and 9.7 ± 0.9 nm which correspond respectively to a maximum of 11.6 and 12.5 monolayers of grafted diazonium.

Fig. 6 displays infrared spectra of NiTi|Py-PD 2eq and 10 eq. Absorption bands characteristic of the electrografted Py-PD layers are observed. The band at 1610 $cm^{-1}$ corresponds to C=C stretching vibrations of the benzene moieties [73]. The bands at 1513 and 1332 $cm^{-1}$ are attributed to C—N interring stretching contributions [73]. Absorption bands around 1160 $cm^{-1}$ are generally attributed to aromatic in-plane C-H deformation [74]. However, these bands are also characteristic of C-O stretching deformation of alcohol groups [74] and could thus be also attributed to the presence of some residual ethanol used for substrates cleaning after polishing and after modification.

The LSV curves (Fig. 7) show a cathodic shift of the corrosion potential ($E_{corr}$) for NiTi modified in the 2 and 10 eq conditions compared to bare NiTi. Similar corrosion current density to bare NiTi is recorded for NiTi|Py-PD 10 eq. However, a decrease of the $j_{corr}$ by one order of magnitude with a mixed inhibition is observed

**Table 1**
Abundance ratios calculated on the basis of XPS analysis of bare NiTi, NiTi|Py-A, NiTi|Py-PD 10 eq, NiTi|Py-PD 2 eq, NiTi|Py-PD 2 eq and bare NiTi after CV from 0 to 1.2 to −1 V/SCE at 50 mV/s for 10 cycle and NiTi|Py-PD 2 eq after 30 minutes at 1.2 V/SCE in 0.1 M $LiClO_4$ in ACN.

| Conditions | Ti/ (Ni + Ti) | C/ (Ni + Ti) | NPy/ (Ni + Ti) | C/ $N_{Py}$ | $N_{Py}$/ $N_{NH2}$ |
|---|---|---|---|---|---|
| Bare NiTi | 0.60 | 0.80 | 0 | 0 | 0 |
| NiTi\|Py-A | 0.60 | 0.93 | 0.04 | 21.8 | 1.0 |
| NiTi\|Py-PD 10 eq | 0.72 | 82.2 | 7.5 | 10.8 | 2.2 |
| NiTi\|Py-PD 2 eq | 0.79 | 46.1 | 4.6 | 10.7 | 3.2 |
| NiTi\|Py-PD 2 eq after CV | 0.75 | 43.2 | 3.7 | 11.6 | 2.2 |
| NiTi\|Py-PD 2 eq after 30 min at 1.2 V/SCE | 0.97 | 4.9 | 0.3 | 15.8 | 2.1 |
| Bare NiTi after CV | 0.76 | 0.69 | 0 | 0 | 0 |

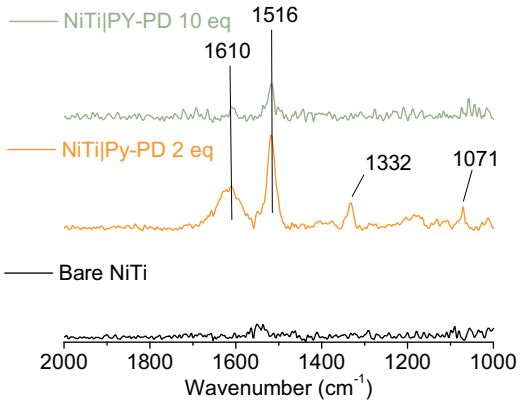


**Fig. 6.** PM-IRRAS spectra of bare NiTi, NiTi|Py-PD 2 eq and NiTi|Py-PD 10 eq.

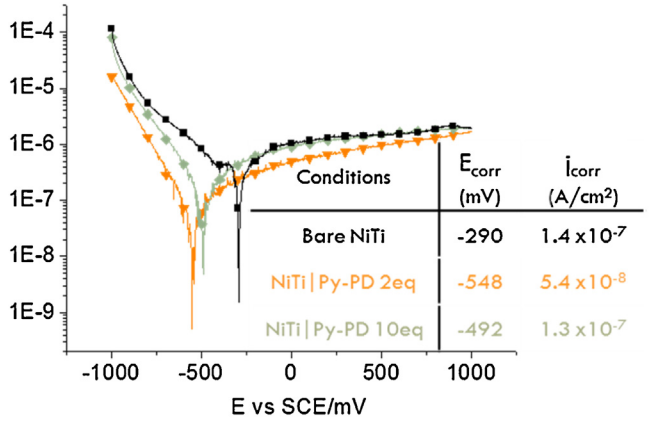


**Fig. 7.** LSV curves for bare NiTi (-■-) NiTi|Py-PD 2 eq (-▼-) and NiTi|Py-PD 10 eq (-♦-).

for NiTi|Py-PD 2 eq. So, for NiTi|Py-PD 2 eq the corrosion resistance is improved despite the grafting of a non-compact organic layer. The lower corrosion resistance in the case of NiTi|Py-PD 10 eq compared to NiTi|Py-PD 2 eq is probably due to defects or a change in the nature (compare to NiTi|Py-PD 2 eq) of the grafted film linked to the side reactions already evidenced by XPS for this condition.

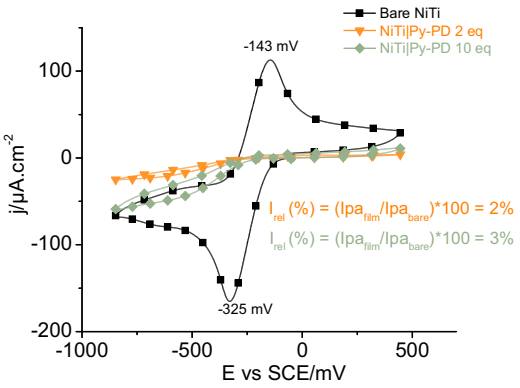


**Fig. 8.** Cyclic voltammetry for bare NiTi (-■-) and NiTi|Py-PD 2 eq (-▼-) and NiTi|Py-PD 10 eq (-♦-) in a 5 mM $Ru(NH_3)_6Cl/0.1$ M $K_2SO_4$ at scan rate of 20 mV/s.

The barrier properties of the grafted organic layers were electrochemically assessed using cyclic voltammetry and $Ru(NH_3)_6Cl_3$ as a redox probe. The CV (Fig. 8) shows a strong inhibition for NiTi|Py-PD 2 eq and 10 eq samples with $I_{rel}$ value of 2% and 3%, respectively.

The water contact angle results point out an increase of the hydrophobicity after substrate modification with the electrografted Py-PD with angles of 53°, 74° and 67° for bare NiTi, NiTi|Py-PD 2 eq and NiTi|Py-PD 10 eq respectively. This increase is less important for NiTi|Py-PD 10 eq than for NiTi|Py-PD 2 eq. This result indicates differences between the two grafted films in agreement with the hypothesis of side-reaction as judged from XPS analyses. A more hydrophilic film for NiTi|Py-PD 10 eq compared to NiTi|Py-PD 2 eq is also in agreement with the LSV results (i.e. a global improvement of the corrosion resistance only for NiTi|Py-PD 2 eq).

To conclude this part, the electrografting of Py-PD on NiTi leads to the formation of multilayers and the titanium dioxide layer at surface of NiTi has been preserved. XPS results indicate probable side reactions (i.e. nitration and chlorination) during the Py-PD generation/grafting for the 10 eq condition. Consequently, NiTi|Py-PD 10 eq presents a corrosion resistance less important and is more hydrophilic than NiTi|Py-PD 2 eq. In regard of these results, the 2 eq condition has been choosen in the sequel of this work to study the grafting of Py-PD without electrochemistry.

### 3.2. Py-PD grafted on NiTi without electrochemistry

The grafting of Py-PD *in situ* generated with 2 eq of $HClO_4$ has been performed at room temperature (SP), under induction heating (IH) and under conventional heating (CH). For the sake of clarity, XPS high resolution N1 s spectra are presented only for NiTi|Py-PD IH80 and NiTi|Py-A SP samples which are representative of all the substrates modified in presence of *in situ* generated Py-PD and in presence of Py-A respectively (Fig. 9). N1 s spectra point out to a successful grafting for the Py-PD condition with a $N_{Py}$ component more significant than the $N_{NH2}$ component while for the Py-A condition physisorbed Py-A is observed. Indeed, as for physisorbed Py-A both components ($N_{Py}$ and $N_{NH2}$) are equal. The C/(Ni + Ti) and $N_{Py}$/(Ni + Ti) (Fig. 10) ratios confirm this result with much lower ratio for Py-A condition compared to Py-PD condition and $N_{Py}/N_{NH2}$ XPS ratio equal to 1 for all NiTi|Py-A substrates

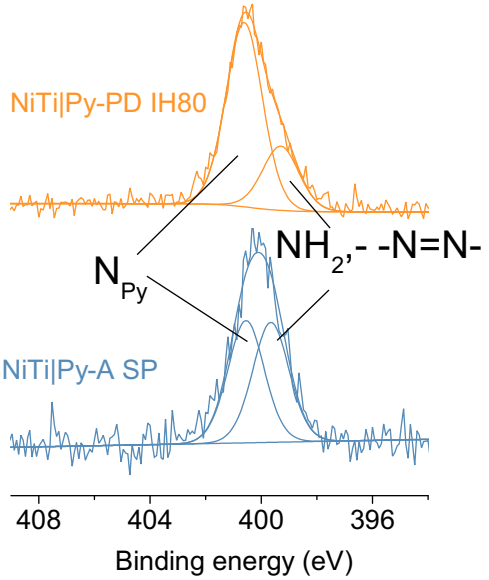


**Fig. 9.** XPS core level spectra of N1 s for NiTi|Py-PD IH80 and NiTi|Py-PD SP substrates.

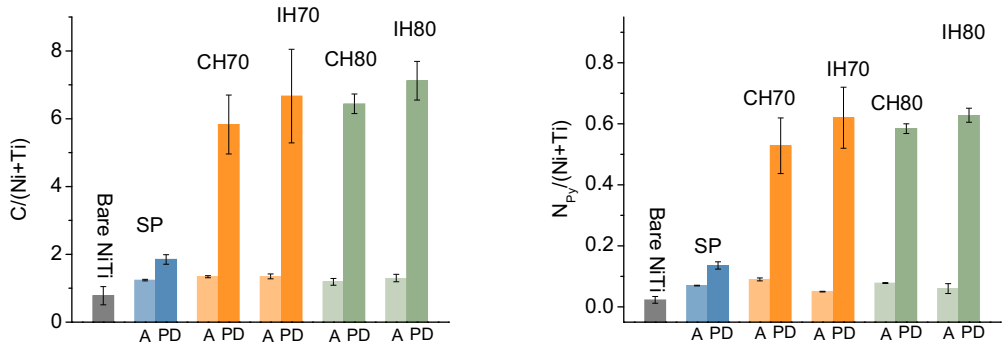


**Fig. 10.** XPS C/(Ni + Ti) and $N_{Py}$/(Ni + Ti) ratio for NiTi|Py-PD (dark colours) and NiTi|Py-A (light colour) modified at room temperature (SP, blue), at 70 °C (orange) at 80 °C (green) by CH or IH.

whatever the heating condition (SP,CH/IH at 70 or 80 °C). As a matter of fact, grafted amount of Py-PD increases with the temperature and is more important for IH compared to CH at the same temperature. Nevertheless, the covering ratio (C/(Ni + Ti) and NPy/(Ni + Ti)) is lower for Py-PD grafted without electrochemistry compared to electrografted Py-PD. This result is in agreement with the calculated thickness which is more or less 4 nm for all the grafted substrates using CH or IH and 2.4 ± 0.29 nm for NiTi|Py-PD SP. The hypothesis of a grafting with a cationic intermediate can be made. Indeed, as mentioned previously the surface of NiTi is oxidized and mainly composed of a $TiO_2$ thin layer preventing the use of NiTi as electron source. Furthermore, the fact that the grafting with a cationic intermediate is thermally activated is in good agreement with the results [24,32]. The slight increase of the grafted amount when IH is used instead of CH seems logical since with IH the cationic intermediate is generated directly at the desired modification area and is less ready to react with the environment. The use of CH and IH appears as a simple and suitable alternative for the modification of substrates without electrochemistry and without reducing agent if the substrate is not reductant. Nevertheless, this observation should be carefully analysed. Indeed, this grafting involves probably a cationic intermediate which is similar to a Wheland intermediate and as mentioned previously Py-PD is highly conjugated and could lead to a better stabilization.

Contact angle measurements as the XPS measurement (values from 73 to 76°) for Py-PD grafted without electrochemistry are in line with the results for Py-PD electrografted. Hence, an increase of the hydrophobicity in agreement with the grafting of aromatic compounds is observed.

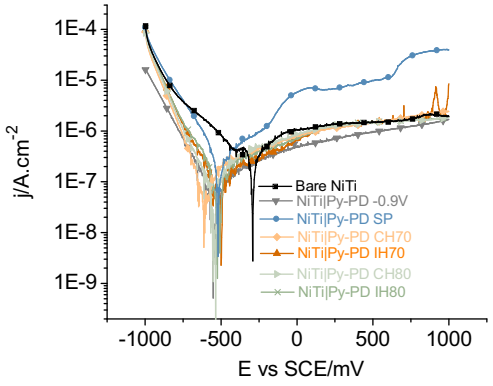


**Fig. 11.** Polarization curves for bare NiTi (-■-),NiTi|Py-PD 2eq (-▼-), NiTi|PyPD SP (-●-),NiTi|Py-PD CH70 (-♦-),NiTi|Py-PD IH70 (-▲-),NiTi|Py-PD CH80 (-▶-) and NiTi|Py-PD IH80 (-X-).

**Table 2**
$E_{corr}$, $j_{corr}$ for bare NiTi, NiTi|Py-PD 2eq, NiTi|PyPD SP, NiTi|PyPD CH70, NiTi|PyPD IH70, NiTi|PyPD CH80, NiTi|PyPD IH80 substrates.

| Conditions | $E_{corr}$ (mV) | $j_{corr}$ (A/cm$^2$) |
|---|---|---|
| Bare NiTi | −290 | $1.4 \times 10^{-7}$ |
| NiTi\|Py-PD −0.9V | −548 | $5.4 \times 10^{-8}$ |
| NiTi\|Py-PD SP | −521 | $2.2 \times 10^{-7}$ |
| NiTi\|Py-PD CH70 | −604 | $9.9 \times 10^{-8}$ |
| NiTi\|Py-PD IH70 | −509 | $6.7 \times 10^{-8}$ |
| NiTi\|Py-PD CH80 | −552 | $6.7 \times 10^{-8}$ |
| NiTi\|Py-PD IH80 | −521 | $5.5 \times 10^{-8}$ |

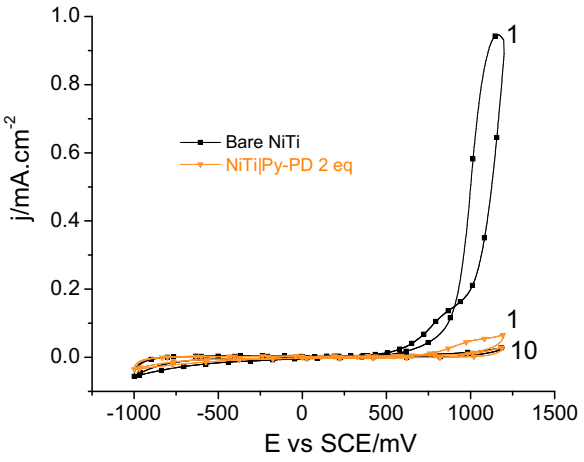


**Fig. 12.** Cyclic voltammetry in monomer-free electropolymerization condition for bare NiTi (-■-) and NiTi|Py-PD 2 eq (-▼-).

The LSV analysis (Fig. 11) shows a cathodic shift of the corrosion potential (Table 2) for the substrates obtained after the grafting of Py-PD for all the heating conditions (CH and IH). All the thermally-assisted modified substrates (CH and IH) present a cathodic reaction inhibition and a decrease of the corrosion current density (Table 2) associated with a slight decrease of the anodic part. In conclusion, there is a global improvement of the corrosion behavior for substrate modified by heating (CH and IH). However, NiTi|Py-PD SP sample shows an increase of the recorded corrosion current densities associated with an increase of the anodic part. This enhancement of the corrosion reaction is probably due to an inhomogeneous modification and a partial grafting of the Py-PD layer at the surface of NiTi (cf. XPS).

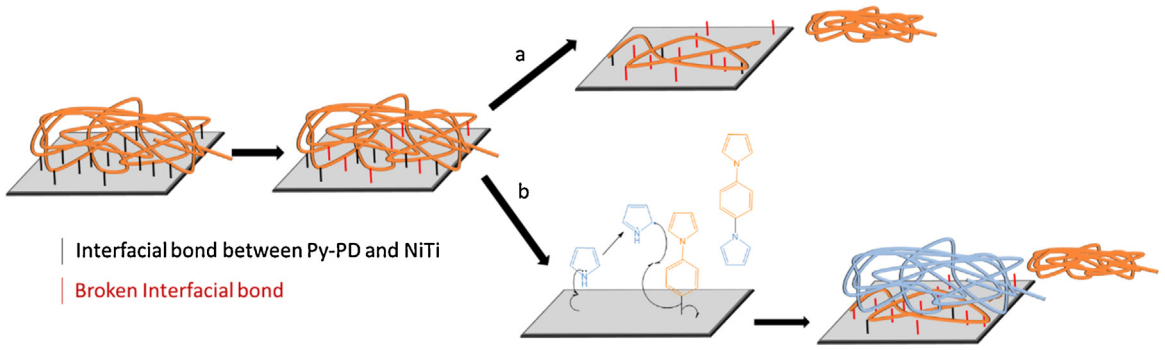


**Fig. 13.** Schematic representation of the grafted Py-PD film (in orange) destruction at the interface with NiTi after the CV (middle part), the potentiostatic (right part a) experiments in the PPy (in blue) electropolymerization condition without Py and during the Py electropolymerization by CV (right part b).

### 3.3. Electropolymerisation of pyrrole on bare NiTi and NiTi|Py-PD 2 eq

Prior to the pyrrole electropolymerization, a comparative electrochemical evaluation between bare NiTi and NiTi|Py-PD 2 eq has been performed in a pyrrole free solution by CV. Fig. 12 shows for bare NiTi an important oxidation peak starting at 400 mV attributed to Ni oxidation [55] and dissolution. Indeed, evaluation by XPS of the surface (Table 1) shows an increase of the titanium content with a Ti/(Ni + Ti) ratio increasing from 0.60 to 0.76. The current density recorded decreases dramatically with the number of cycles indicating a reinforcement of the protective titanium oxide surface layer. The CV for NiTi|Py-PD presents an oxidation peak starting at 500 mV, this higher potential compared to that of bare NiTi confirms the protective role of the grafted Py-PD. As for bare NiTi this oxidation wave is attributed to Ni oxidation but at a lower rate since the recorded current densities are one order lower which highlights again the protective role of the grafted Py-PD. Furthermore, oxidation of the pyrrole function from grafted Py-PD in this range of potential cannot be excluded. The XPS ratios (C/(Ni + Ti) and $N_{Py}$/(Ni + Ti)) (Table 1) show a partial destruction (i.e. a slight decrease of the recorded ratios) of the grafted film due to the oxidation of Ni and the partial destruction of the bonds between the grafted film and the NiTi surface (as shown on Fig. 13 middle part). The free monomer electropolymerization conditions without pyrrole have been evaluated in potentiostatic conditions at 1.2 V/SCE for 30 min which are harsher conditions. In this condition, a dramatic decrease of the covering rate is observed (C/(Ni + Ti) and $N_{Py}$/(Ni + Ti)) (Table 1) with a major film desorption (as schematically shown on Fig. 13 right part a) due to a continuous oxidation of the Ni and so of the surface oxide layer dissolution at this potential [55]. This hypothesis is supported by the Ti/(Ni + Ti) ratio indicating the almost complete disappearance of nickel at the surface of NiTi. Consequently, in the sequel of this work, to avoid the destruction of the grafted adhesion promoter layer, the electropolymerization of pyrrole is carried out in CV condition.

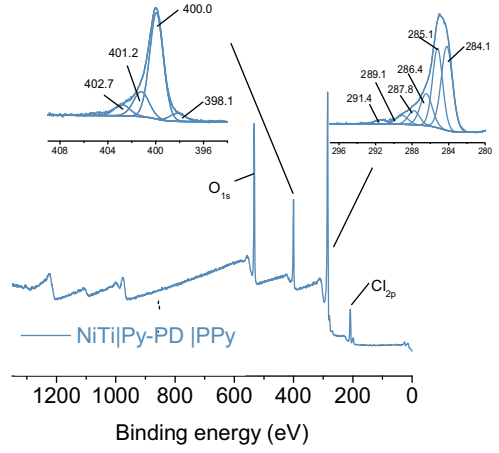


**Fig. 15.** XPS survey and core level spectra of N1 s and C1 s for NiTi|Py-PD|PPy.

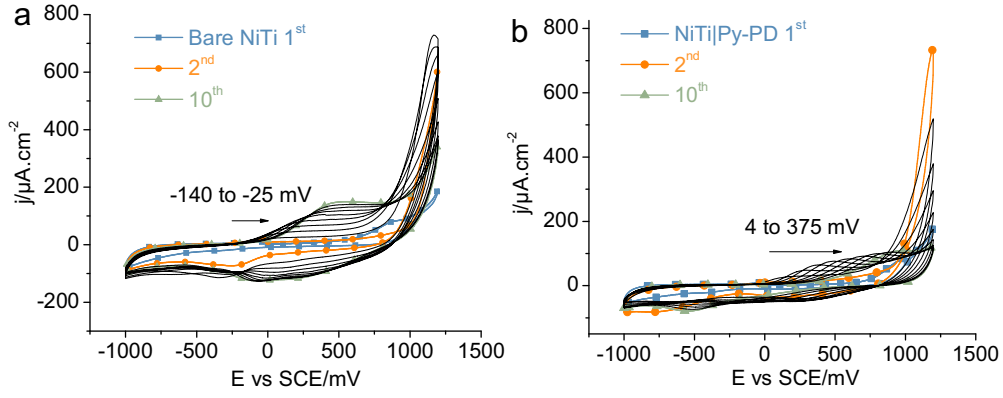


**Fig. 14.** CV of the electropolymerization of Py in an acetonitrile 1 mM Py and 0.1 M $LiClO_4$ solution the 1st (-■-), 2nd (-●-) and 10th (-▲-) cycle on bare NiTi (a) and on NiTi|Py-PD (b).

Pyrrole electropolymerization (Fig. 14) CV for both NiTi|Py-PD and bare Ni present the classical behaviour recorded for the electropolymerization of conducting polymers. Indeed, two oxidation waves corresponding to Ni oxidation (as mention previously for CV recorded without Py) and the pyrrole monomer oxidation (≈1100 mV for both substrates) are present at anodic potential during the first cycle. For the others cycles, two parts are also observed but with other attributions. The first at lower potential (than monomer oxidation) corresponds to the polymer oxidation and reduction with a current density increasing with the number of cycles due to the polymer growth. The other one, at more anodic potential, corresponds to the monomer oxidation but also to oligomers present in solution after the first cycle (product of oxidized monomer coupling). The decrease of the potential for the second oxidation wave after the first cycle is due to the presence of these easier oxidizable oligomers in the solution.

The increase of the recorded oxidation potential of the polymer for both substrates with the number of cycle is symptomatic of short and poor quality polymer. The decrease of the current densities recorded for the oxidation of the monomer between the 2nd and 10th is a consequence of the poor quality of the film.

For NiTi|PPy and NiTi|Py-PD|PPy a visual removal of the film is observed when the substrates are cleaned in the sonication bath. Nevertheless, this removing of the PPy film is slower for NiTi|Py-PD|PPy.

The XPS spectra are presented only for NiTi|Py-PD|PPy in Fig. 15. The results for NiTi|PPy are not shown because the PPy films do not withstand the vacuum in the XPS chamber which is another qualitative information on the better adhesion of electropolymerised pyrrole on substrate modified with the Py-PD adhesion promoter. The survey spectra for NiTi|Py-PD|PPy shows an increase of the $C_{1s}$ and $N_{1s}$ peak intensity compared to bare NiTi which confirms the presence of the PPy film and the appearance of the $Cl_{2p}$ peak. The presence of chlorine is due to the insertion of perchlorate ions during the film formation and oxidation. Another difference for the NiTi|Py-PD|PPy sample is the disappearance of the Ti characteristic peaks in agreement of the thickness measurement recorded by mechanic profilometry of 307 ± 220 nm higher, than the sampling depth of the XPS (10 nm).

The $C_{1s}$ peak (Fig. 15 inset) can be analysed using six different components at 284.1, 285.1, 286.4, 287.8, 289.1 and 291.4 eV. The two peaks at the lowest binding energies correspond to β-carbons (C-C) and α-carbon (C-N) in the pyrrole, respectively [45]. The peak at 286.4 eV is attributed to carbons involved in polaron (C-NH+) [45,75] or C-O bond from oxidized polymer or trapped rinsing solvent. The peak at 287.8 eV is assigned to bipolaron (C=NH+) [45,75]. The peak at 289.1 eV could be related to ester groups (C=O) [26,76]. The 286.4, 287.8 and 289.1 eV peaks are characteristics of oxidised pyrrole film and are in agreement with the previous results. Ultimately, at 290.8 eV the shake-up satellite peak characteristic of an aromatic is observed [27,45].

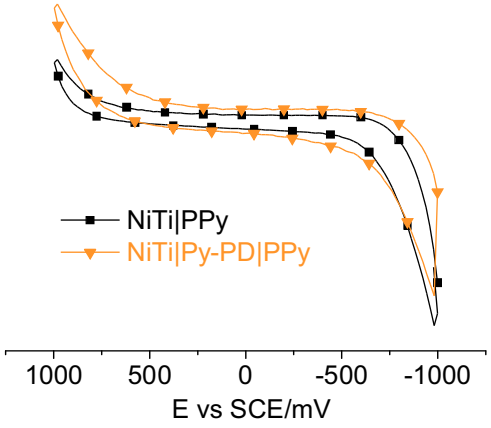


**Fig. 16.** Open circuit potential ($E_{OC}$) for bare NiTi (-■-), NiTi|PPy (-●-), NiTi|Py-PD (-▼-), NiTi|Py-PD|PPy (-▲-).

**Table 3**
Abundance ratios calculated on the basis of XPS analysis of bare NiTi, NiTi|Py-PD, NiTi|Py-PD|PPy, NiTi|Py-PD|PPy after sonication NiTi|Py-PD|PPy$^{s}$ and NiTi|Py-PD|PPy after peeling test NiTi|Py-PD|PPy$^{p}$.

| Conditions | Ti/(Ni + Ti) | C/(Ni + Ti) | N/(Ni + Ti) | C/N |
|---|---|---|---|---|
| Bare NiTi | 0.60 | 0.80 | 0.02 | 34.8 |
| NiTi|Py-PD | 0.79 | 46.1 | 6.12 | 10.7 |
| NiTi|Py-PD|PPy | / | / | / | 4.9 |
| NiTi|Py-PD|PPy$^{s}$ | 0.74 | 0.86 | 0.06 | 14.1 |
| NiTi|Py-PD|PPy$^{s}$ | 0.76 | 0.91 | 0.07 | 12.1 |

The nitrogen peak analysis is consistent with the XPS results on C. The $N_{1s}$ peaks (Fig. 15 inset) is analysed using 3 components at 400.0, 401.2 and 402.6 eV corresponding to amine like bonds of pyrrole (N-H), to positively charged nitrogens (-$NH^{+}$) (polaron) and to oxidized nitrogens (bipolaron) (=$NH^{+}$) respectively [45,77].

Typical doping/dedoping CV graphs (not presented) for the NiTi|Py-PD|PPy and NiTi|PPy show a weak capacitive current and do not show the typical oxidation and reduction of the polymer layer inducing counter-ions transfers inside and outside the layer (doping and dedoping) [78]. This behaviour similar to insulating polymer reflects the poor quality of the PPy film inducing its loss of conductivity and it is in agreement with CV recorded during the PPy film formation.

The open circuit potential ($E_{OC}$) measurements for NiTi substrates (Fig. 16) show a decrease of the $E_{OC}$ (after 1 h) from ~ –345 mV to ~ –430 mV for Ni|Py-PD compared to bare Ni. This shift towards more cathodic $E_{OC}$ is in agreement with the previous $E_{corr}$ cathodic shift recorded from the LSV measurement. The $E_{OC}$ for NiTi|Py-PDPPy ~ 30 mV (after 1 h) shows an ennoblement of the substrate. An increase of $E_{OC}$ with time is observed which indicates the absence of galvanic coupling between the oxidized PPy film and the NiTi substrate [79–81] and is another indication of the conductivity loss and so of the poor quality of the PPy film. Similar conclusions can be made for NiTi|PPy sample but with a less important ennoblement ($E_{OC}$ of ~–40 mV) compared to NiTi|Py-PD|PPy.

While the PPy film is completely non-adherent on bare NiTi, the adherence of the PPy film electropolymerized on NiTi|Py-PD sample has been evaluated by XPS after its sonication and after a peeling tests (ASTM D3359). Results are presented in Table 3. For NiTi|Py-PD|PPy a successful polymerisation of the PPy with C/N ratio close to the theoretical ratio of 4 for a pure PPy film is observed. The excess of carbon is due to atmospheric contaminations. After both the sonication and the peeling test, a complete removal of the PPy film but also of the adhesion promoter layer is observed. Indeed, C/(Ni + Ti), and N/(Ni + Ti) ratios are close to the ratios recorded for bare NiTi and far under the ratios recorded for NiTi|Py-PD. As mentioned previously in the CV condition for the electropolymerization of pyrrole dissolution of metallic species occurs [55] and consequently a partial destruction of the bonds between the Py-PD and the NiTi (Fig. 13 middle part). In presence of pyrrole, pyrrole radicals are generated at the electrode surface near the interfacial bond between grafted Py-PD and NiTi, these pyrrole radicals probably react with the grafted Py-PD leading to another partial destruction of the Py-PD film (Fig. 13 right part b). Finally, both reactions (i.e. metallic species dissolution at anodic potential and radical pyrrole reaction with the interfacial bond between grafted Py-PD and NiTi) lead to the almost complete destruction of the adhesion promoter layer and to the formation of PPy film

mainly physisorbed. To avoid this phenomenon the experiments have been carried out with lower concentration of Py (i.e. 0.1 mM and 0.01 mM) but with these concentrations the electropolymerization doesn't occur. A solution could be to increase the final potential (which is at 1.2 V/ECS) but then the decrease of the Py-PD destruction (due to the reaction between radical pyrrole and the interfacial bond) thanks to the decrease of the Py concentration will be compensated by the increase of metallic species dissolution.

## 4. Conclusions and outlooks

The electrografting of Py-PD on NiTi has been successfully achieved with two acidic (i.e. 2 and 10 eq of $HClO_4$) conditions for its *in situ* generation. In both cases, the surface of NiTi has been preserved. Hence, hypotheses on the bond at the interface between NiTi and the grafted film have been proposed and partially verified with the presence of C—N=N-O-Ni bond. NiTi|Py-PD 2eq and NiTi-Py-PD 10 eq. present high coverage ratios with multilayers formation. XPS results indicate probable side reactions (i.e. nitration and chlorination) during the Py-PD generation/grafting for the 10 eq condition. Consequently, NiTi|Py-PD 10 eq presents a corrosion resistance less important than NiTi|Py-PD 2 eq and NiTi|Py-PD 10 eq is more hydrophilic than NiTi|Py-PD 2 eq. Therefore, beyond the interest to use gentle acidic conditions (i.e. 2 eq of $HClO_4$) for the *in situ* generation of diazonium salts to avoid detrimental effect on the surface of sensitive oxidizable metals (which are not observed here since the electrografting of Py-PD with 10 eq of $HClO_4$ has been successfully achieved), this condition avoids side-reaction during the grafting of diazonium salts. Hence, the 2 eq of acid condition should be preferred or at least used when the diazonium *in situ* generation is problematic.

The grafting of Py-PD *in situ* generated on NiTi has been also achieved at room temperature and thermally assisted (IH and CH at 70 or 80 °C). The grafted film shows similar properties to the film obtained by electrografting (cf. XPS, contact angle and LSV) but with a lower thickness. The NiTi|Py-PD SP shows a lower coverage compared to the substrate modified by CH and IH which is in agreement with the formation of a cationic intermediate thermally activated.

Finally, the electropolymerization of Py has been successfully achieved providing conductive polymer top coat, probably attached via electrostatic interactions to the underlying NiTi-Py-PD. This mechanism of adhesion is probably driven by the concomitant oxidation of metallic species and the reaction of pyrrole radical with the grafted Py-PD inducing the failure of the interfacial bond between grafted Py-PD and NiTi. We have also noted that the conductive polymer top coat fails only under extreme adhesion testing conditions such as ultrasonication. Nevertheless, Py-PD could be used as a coupling agent for the electrodeposited polypyrrole, with reasonably good adhesion therefore ensuring substantial corrosion resistance of Nitinol.

## References


[1] F. El Feninat, G. Laroche, M. Fiset, D. Mantovani, Shape memory materials for biomedical applications, Adv. Eng. Mater. 4 (2002) 91–104.
[2] W.J. Buehler, R.C. Wiley, Nickel-Base Allaoy, U.S. Patent US3174851, 1965.
[3] M.H. Elahinia, M. Hashemi, M. Tabesh, S.B. Bhaduri, Manufacturing and processing of NiTi implants: A review, Prog. Mater. Sci. 57 (2012) 911–946.
[4] S.A. Shabalovskaya, Surface, corrosion and biocompatibility aspects of Nitinol as an implant material, Biomed. Mater. Eng. 12 (2002) 69–109.
[5] T. Duerig, A. Pelton, D. Stöckel, An overview of nitinol medical applications, Mater. Sci. Eng. A 273–275 (1999) 149–160.
[6] D. Stoeckel, Nitinol medical devices and implants, Minim. Invasive Ther. Allied Technol. 9 (2000) 81–88.
[7] J. Mohd Jani, M. Leary, A. Subic, M.A. Gibson, A review of shape memory alloy research, applications and opportunities, Mater. Des. 56 (2014) 1078–1113.
[8] T. Duerig, A. Pelton, D. Stöckel, An overview of nitinol medical applications, Mater. Sci. Eng. A 273–275 (1999) 149–160.
[9] G. Rondelli, Corrosion resistance tests on NiTi shape memory alloy, Biomaterials 17 (1996) 2003–2008.
[10] Z. Bai, H.H. Rotermund, The intrinsically high pitting corrosion resistance of mechanically polished nitinol in simulated physiological solutions, J. Biomed. Mater. Res. B. Appl. Biomater. 99 (2011) 1–13.
[11] S.A. Shabalovskaya, G.C. Rondelli, A.L. Undisz, J.W. Anderegg, T.D. Burleigh, M.E. Rettenmayr, The electrochemical characteristics of native Nitinol surfaces, Biomaterials 30 (2009) 3662–3671.
[12] X. Lü, X. Bao, Y. Huang, Y. Qu, H. Lu, Z. Lu, Mechanisms of cytotoxicity of nickel ions based on gene expression profiles, Biomaterials 30 (2009) 141–148.
[13] J.L. Bahr, J.M. Tour, Highly functionalized carbon nanotubes using in situ generated diazonium compounds, Chem. Mater. 13 (2001) 3823–3824.
[14] J. Pinson, Attachement of organic layers to materials surfaces by reduction of diazonium salts, in: M.M. Chehimi (Ed.), Aryl Diazonium Salts, Wiley, New-York, 2012, pp. 1–27.
[15] E. Lebègue, T. Brousse, C. Cougnon, Spontaneous arylation of activated carbon from aminobenzene organic acids as source of diazonium ions in mild, Electrochim. Acta 88 (2013) 680–687.
[16] J. Pinson, R. Hitmi, J.-M. Saveant, European Patent EP0569503, (1992).
[17] D. Bélanger, J. Pinson, Electrografting: a powerful method for surface modification, Chem. Soc. Rev. 40 (2011) 3995–4048.
[18] A. Chausse, M.M. Chehimi, N. Karsi, J. Pinson, F. Podvorica, C. Vautrin-Ul, The Electrochemical Reduction of Diazonium Salts on Iron Electrodes. The Formation of Covalently Bonded Organic Layers and Their Effect on Corrosion, Chem. Mater. 14 (2002) 392–400.
[19] K. Boukerma, M.M. Chehimi, J. Pinson, C. Blomfield, X-ray photoelectron spectroscopy evidence for the covalent bond between an iron surface and aryl Groups attached by the electrochemical reduction of diazonium salts, Langmuir 19 (2003) 6333–6335.
[20] Y.A. Atmane, L. Sicard, A. Lamouri, J. Pinson, M. Sicard, C. Masson, et al., Functionalization of Aluminum Nanoparticles Using a Combination of Aryl Diazonium Salt Chemistry and Iniferter Method, J. Phys. Chem. C 117 (2013) 26000–26006.
[21] G. Chamoulaud, D. Belanger, Spontaneous Derivatization of a Copper Electrode with in Situ Generated Diazonium Cations in Aprotic and Aqueous Media, J. Phys. Chem. C 111 (2007) 7501–7507.
[22] D. Quinton, A. Galtayries, F. Prima, S. Griveau, Functionalization of titanium surfaces with a simple electrochemical strategy, Surf. Coatings Technol. 206 (2012) 2302–2307.
[23] B.L. Hurley, R.L. McCreery, Covalent Bonding of Organic Molecules to Cu and Al Alloy 2024 T3 Surfaces via Diazonium Ion Reduction, J. Electrochem. Soc. 151 (2004) B252–259.
[24] A. Mesnage, X. Lefèvre, P. Jégou, G. Deniau, S. Palacin, Spontaneous grafting of diazonium salts: chemical mechanism on metallic surfaces, Langmuir 28 (2012) 11767–11778.
[25] A.A. Mohamed, Z. Salmi, S.A. Dahoumane, A. Mekki, B. Carbonnier, M.M. Chehimi, Functionalization of nanomaterials with aryldiazonium salts, Adv. Colloid Interface Sci. (2015) 2–8.
[26] A. Jacques, S. Devillers, B. Arrotin, J. Delhalle, Z. Mekhalif, Polyelectrolyte Multilayers Deposition on Nitinol Modified by In Situ Generated Diazonium in Gentle Conditions, J. Electrochem. Soc. 161 (2014) G55–G62.
[27] A. Jacques, S. Devillers, J. Delhalle, Z. Mekhalif, Electrografting of In Situ Generated Pyrrole Derivative Diazonium Salt for the Surface Modification of Nickel, Electrochim. Acta. 109 (2013) 781–789.
[28] A. Jacques, B. Barthélémy, J. Delhalle, Z. Mekhalif, Nitinol Modified by In Situ Generated Diazonium from Its Nitro Precursor for the SI-ATRP of 2-Hydroxyethyl Methacrylate, J. Electrochem. Soc. 162 (2015) G94–G102.
[29] S. Baranton, D. Bélanger, Electrochemical derivatization of carbon surface by reduction of in situ generated diazonium cations, J. Phys. Chem. B 109 (2005) 24401–24410.
[30] A. Adenier, N. Barré, E. Cabet-Deliry, A. Chaussé, S. Griveau, F. Mercier, et al., Study of the spontaneous formations of organic layers on carbon and metal surfaces from diazonium salts, Surf. Sci. 600 (2006) 4801–4812.
[31] M. Toupin, D. Bélanger, Spontaneous functionalization of carbon black by reaction with 4-nitrophenyldiazonium cations, Langmuir 24 (2008) 1910–1917.
[32] P. Abiman, G.G. Wildgoose, R.G. Compton, A mechanistic investigation into the covalent chemical derivatisation of graphite and glassy carbon surfaces using aryldiazonium salts, J. Phys. Org. Chem. 21 (2008) 433–439.
[33] R. Pazo-llorente, C. Bravo-diaz, E. Gonzalez-romero, pH Effects on Ethanolysis of Some Arenediazonium Ions: Evidence for Homolytic Dediazoniation Proceeding through Formation of Transient Diazo Ethers, (2004), 3221–3226.
[34] Q. Li, C. Batchelor-McAuley, N.S. Lawrence, R.S. Hartshorne, R.G. Compton, The synthesis and characterisation of controlled thin sub-monolayer films of 2-anthraquinonyl groups on graphite surfaces, New J. Chem. 35 (2011) 2462.
[35] J. Clayden, N. Greeves, S. Warren, P. Wothers, In organic chemistry (2001).
[36] J.A. William, Les amines, in: Invit. À La Chim. Org., 2003: p. 418.
[37] E. Lebègue, L. Madec, T. Brousse, J. Gaubicher, E. Levillain, C. Cougnon, Modification of activated carbons based on diazonium ions in situ produced from aminobenzene organic acid without addition of other acid, J. Mater. Chem. 21 (2011) 12221–12223.
[38] S. Devillers, B. Barthélémy, J. Delhalle, Z. Mekhalif, Induction Heating Vs Conventional Heating for the Hydrothermal Treatment of Nitinol and Its Subsequent 2- (Methacryloyloxy) ethyl 2- (trimethylammonio) ethyl

Phosphate Coating by Surface-Initiated Atom Transfer Radical Polymerization, Appl. Mater. Interfaces 3 (2011) 4059–4066.
[39] B. Arrotin, A. Jacques, S. Devillers, J. Delhalle, Z. Mekhalif, Induction heating to trigger the nickel surface modification by in situ generated 4- carboxybenzene diazonium, Appl. Surf. Sci. 370 (2016) 320–327.
[40] A. Vacca, M. Mascia, S. Rizzardini, S. Palmas, L. Mais, Coating of gold substrates with polyaniline through electrografting of aryl diazonium salts, Electrochim. Acta 126 (2014) 81–89.
[41] L. Pilan, M. Raicopol, A. Pruna, V. Branzoi, Polyaniline/carbon nanotube composite films electrosynthesis through diazonium salts electroreduction and electrochemical, Surf. Interface Anal. 44 (2012) 1198–1202.
[42] S. Descroix, G. Hallais, C. Lagrost, J. Pinson, Electrochimica Acta Regular poly (para −phenylene) films bound to gold surfaces through the electrochemical reduction of diazonium salts followed by electropolymerization in an ionic liquid, Electrochim. Acta 106 (2013) 172–180.
[43] B. Bouktit, Z. Salmi, P. Decorse, M. Jouini, D. Aswal, A. Singh, et al., Polypyrrole/Ag nanocomposite films on diazonium salt modified indium tin oxide substrate, J. Colloid Sci. Biotechnol. 2 (2013) 200–210.
[44] P. Herrasti, P. Oco, Polypyrrole layers for steel protection, Appl. Surf. Sci. 172 (2001) 276–284.
[45] F. Lallemand, D. Auguste, C. Amato, L. Hevesi, J. Delhalle, Z. Mekhalif, Electrochemical synthesis and characterization of N-substituted polypyrrole derivatives on nickel, Electrochim. Acta 52 (2007) 4334–4341.
[46] T. Tüken, G. Arslan, B. Yazıcı, M. Erbil, The corrosion protection of mild steel by polypyrrole/polyphenol multilayer coating, Corros. Sci. 46 (2004) 2743–2754.
[47] T. Tüken, B. Yazıcı, M. Erbil, Polypyrrole films on nickel-plated copper, Prog. Org. Coatings 54 (2005) 372–376.
[48] B. Garner, A. Georgevich, A.J. Hodgson, L. Liu, G.G. Wallace, G.E.T. Al, Polypyrrole −heparin composites as stimulus-responsive substrates for endothelial cell growth, J. Biomed. Mater. Res. 44 (1999).
[49] J.H. Collier, J.P. Camp, T.W. Hudson, C.E. Schmidt, Synthesis and characterization of polypyrrole-hyaluronic acid composite biomaterials for tissue engineering applications, J. Biomed. Mater. Res. 50 (2000) 574–584.
[50] J.Y. Wong, R. Langer, D.E. Ingber, Electrically conducting polymers can noninvasively control the shape and growth of mammalian cells, Proc. Natl. Acad. Sci. U. S. A. 91 (1994) 3201–3204.
[51] E. De Giglio, M.R. Guascito, L. Sabbatin, G. Zambonin, Electropolymerization of pyrrole on titanium substrates for the future development of new biocompatible surfaces, Biomaterials 22 (2001) 2609–2616.
[52] D.D. Ateh, H. Navsaria, P. Vadgama, Polypyrrole-based conducting polymers and interactions with biological tissues, J. R. Soc. Interface 3 (2006) 741–752.
[53] H. Castano, E. a. O'Rear, P.S. McFetridge, V.I. Sikavitsas, Polypyrrole thin films formed by admicellar polymerization support the osteogenic differentiation of mesenchymal stem cells, Macromol. Biosci. 4 (2004) 785–794.
[54] N.K. Guimard, N. Gomez, C.E. Schmidt, Conducting polymers in biomedical engineering, Prog. Polym. Sci. 32 (2007) 876–921.
[55] D.O. Flamini, S.B. Saidman, Electrodeposition of polypyrrole onto NiTi and the corrosion behaviour of the coated alloy, Corros. Sci. 52 (2010) 229–234.
[56] D.O. Flamini, S.B. Saidman, Corrosion behaviour of Nitinol alloy coated with alkylsilanes and polypyrrole, Mater. Sci. Eng. C. Mater. Biol. Appl. 44 (2014) 317–325.
[57] D.J. C, G.J. Cruz, M.G. Olayo, L.M. Gómez, Coatings by plasmas of pyrrole on nitinol and stainless steel substrates, 25, (2012), 157-160.
[58] M. Torabi, S.K. Sadrnezhaad, Corrosion behavior of polypyrrole/hydroxyapatite nanocomposite thin films electropolymerized on NiTi substrates in simulated body fluid, Mater. Corros. 62 (2011) 252–257.
[59] S. Samanta, I. Bakas, A. Singh, D.K. Aswal, M.M. Chehimi, In situ diazonium-modified flexible ITO-coated PEN substrates for the deposition of adherent silver-polypyrrole nanocomposite films, Langmuir 30 (2014) 9397–9406.
[60] P.J. Cumpson, M.P. Seah, Elastic Scattering Corrections in AES and XPS. II. Estimating Attenuation Lengths and Conditions Required for their Valid Use in Overlayer/Substrate Experiments, Surf. Interface Anal. 25 (1997) 430–446.
[61] R.G. Greenler, Infrared Study of Adsorbed Molecules on Metal Surfaces by Reflection Techniques, J. Chem. Phys. 44 (1966) 310–316.
[62] S. Baranton, D. Bélanger, In situ generation of diazonium cations in organic electrolyte for electrochemical modification of electrode surface, Electrochim. Acta 53 (2008) 6961–6967.
[63] D. Gningue-sal, A. Kone, J. Aaron, S. Aeiyach, M. Hedayatullah, P. Lacaze, Poly [(1-methylene-2-methylnaphtalene)-N-pyrrole]: a new fluorophore-containing electroactive conducting polymer, Synth. Met. 82 (1996) 119–127.
[64] R. Schmidt, E. McNellis, W. Freyer, D. Brete, T. Gießel, C. Gahl, et al., Azobenzene-functionalized alkanethiols in self-assembled monolayers on gold, Appl. Phys. A 93 (2008) 267–275.
[65] P. Doppelt, G. Hallais, J. Pinson, F. Podvorica, S. Verneyre, Surface Modification of Conducting Substrates. Existence of Azo Bonds in the Structure of Organic Layers Obtained from Diazonium Salts, Chem. Mater. 19 (2007) 4570–4575.
[66] K. Roodenko, M. Gensch, J. Rappich, K. Hinrichs, N. Esser, R. Hunger, Time-resolved synchrotron xps monitoring of irradiation-induced nitrobenzene reduction for chemical lithography, J. Phys. Chem. B. 111 (2007) 7541–7549.
[67] A.V. Topchiev, Nitration ofof Hydrocarbons and other Organic Compounds, Pergamon P, London, 1959.
[68] V.J.G. Hoggett, R.B. Moodie, J.R. Penton, K. Schofield, Nitration and aromatic reactivity, Angew. Chemie 84 (1972) 1156.
[69] D.R. Lide, CRC Handbook of Chemistry and Physics, CRC Press, 2005.
[70] H. Kominami, H. Gekko, K. Hashimoto, Photocatalytic disproportionation of nitrite to dinitrogen and nitrate in an aqueous suspension of metal-loaded titanium(IV) oxide nanoparticles, Phys. Chem. Chem. Phys. 12 (2010) 15423–15427.
[71] D.T. Clark, D. Kilcast, W.K.R. Musgrave, Molecular core binding energies for some monosubstituted benzenes, as determined by X-ray photoelectron spectroscopy, J. Chem. Soc. D Chem. Commun. 9 (1971) 516b.
[72] M.C. Biesinger, B.P. Payne, B.R. Hart, A.P. Grosvenor, N.S. McIntryre, L.W. Lau, et al., Quantitative chemical state XPS analysis of first row transition metals, oxides and hydroxides, J. Phys. Conf. Ser. 100 (2008) 012025.
[73] D. Schweke, B. Brauer, R.B. Gerber, Y. Haas, The vibrational spectra of N-phenylpyrrole in the gas phase, in argon matrices and in single crystals, Chem. Phys. 333 (2007) 168–178.
[74] G. Socrate, Infrared characterisic group frequencies, 2nd ed., (1994).
[75] A. Jacques, B. Barthélémy, J. Delhalle, Z. Mekhalif, 1-Pyrrolyl-10-decylammoniumphosphonate monolayer: a molecular nanolink between electropolymerized pyrrole films and nickel or titanium surfaces, Electrochim. Acta 170 (2015) 218–228.
[76] S.J. Vigmond, K.M.R. Kallury, M. Thompson, Pyrrole Copolymerization and Polymer Derivatization Studied by X-ray Photoelectron Spectroscopy, (1992), 2763–2769.
[77] E. Jaehne, S. Oberoi, H.-J.P. Adler, Ultra thin layers as new concepts for corrosion inhibition and adhesion promotion, Prog. Org. Coatings 61 (2008) 211–223.
[78] Y.W. Chen-Yang, J.L. Li, T.L. Wu, W.S. Wang, T.F. Hon, Electropolymerization and electrochemical properties of (N-hydroxyalkyl)pyrrole/pyrrole copolymers, Electrochim. Acta 49 (2004) 2031–2040.
[79] D.O. Flamini, S.B. Saidman, Corrosion behaviour of nitinol alloy coated with alkylsilanes and polypyrrole, Mater. Sci. Eng. C 44 (2014) 317–325.
[80] G.M. Spinks, A.J. Dominis, G.G. Wallace, D.E. Tallman, Electroactive conducting polymers for corrosion control: Part 2. Ferrous metals, J. Solid State Electrochem. 6 (2002) 85–100.
[81] G. Williams, H.N. McMurray, Factors Affecting Acid-Base Stability of the Interface Between Polyaniline Emeraldine Salt and Oxide Covered Metal, Electrochem. Solid-State Lett. 8 (2005) B42.